Desalination and Water Treatment
www.deswater.com

doi: 10.5004/dwt.2018.22134

109 (2018) 28–35
March

Performance comparison between TFC-ES membranes and aquaporin membranes for dairy wastewater reclamation

Hongwei Song, Jinrong Liu*, Dou Wu

School of Chemical Engineering, Inner Mongolia University of Technology, Hohhot 010051, China,
emails: jinrong_liu@126.com (J. Liu), sophiesong_0471@hotmail.com (H. Song), 352565955@qq.com (D. Wu)

Received 26 November 2017; Accepted 28 February 2018

ABSTRACT

Real dairy wastewater (DWW) was reclaimed by a hybrid system of forward osmosis and membrane distillation (FO/MD). Two types of thin film composite membranes were employed in this study, one with embedded polyester screen support (TFC-ES), and the other with aquaporin (AQP). Sodium chloride solution (1 M) was used as the draw solution. The hybrid system consisted of a cross-flow FO cell and an air gap MD module. Water flux (J_w), reverse draw solute flux (J_s), and contaminant rejections were analyzed to compare the performances of the TFC-ES membrane and the AQP membrane in individual FO experiments and FO/MD experiments. In addition, specific reverse salt flux (J_s/J_w) was calculated to further illustrate the selectivity of the FO membranes. The specific reverse salt flux of the TFC-ES membrane was much lower and more stable than that of the AQP membrane, which suggested superior flux behavior of the TFC-ES membrane. A fouled TFC-ES membrane could recover 91.79% of the flux in comparison with 81.33% for a fouled AQP membrane after cleaning. Furthermore, contaminant rejections of the AQP membrane were slight higher than that of the TFC-ES membrane.

Keywords: Dairy wastewater reclamation; Hybrid system; Specific reverse salt flux; TFC-ES membrane; AQP membrane

1. Introduction

Wastewater recycling is one of the best ways of alleviating water scarcity and water/wastewater pollution. Non-potable reuse of recycled wastewater is currently the popularity rather than exception in many parts of the world [1]. China has been frequently been confronted with water scarcity, and both central and local governments have issued policies to promote wastewater recycling. In addition, water is intensively consumed in most industrial processes, so complex industrial water/wastewater management has need for a sustainable solution, meaning that industrial wastewater reclamation is significant. The dairy industry is generally regarded as the largest industrial food wastewater source in many countries [2]. With it making rapid developments in recent decades, remarkable progress on dairy production and consumption has been achieved in China. Moreover, in around 50% of the world's whey production (especially concerning acid whey) wastewater is untreated prior to disposal [2]. Anaerobic processes integrated with active sludge processes are a conventional treatment for dairy wastewater (DWW). However, the anaerobic process is costly, complicated and has hidden security dangers. Therefore, it is necessary that more compact and innovative processes be developed to meet stringent wastewater treatment limitations and water quality requirements. Membrane processes play a key role in advanced wastewater reclamation with advantages of producing high water quality and a relatively small footprint. The demand for membranes in China exceeded 4.8 billion dollars in 2010, amounting to about 15% of world total [3]. An innovative membrane process (forward osmosis (FO), which is an osmotic driven process [4] and has low fouling propensity [5–7]) has attracted more and more attention in the course of the last decade [8–13]. FO can directly filter

* Corresponding author.

complex wastewaters, generating freshwater when coupled with a draw solution (DS) recovery process and membrane distillation (MD), a thermally driven process whereby vapor can permeate through a hydrophobic membrane that prevents liquid passing [14,15]. In an FO/MD hybrid system, FO provides a foulant-free solution to MD for the DS recovery so as to produce higher water quality and improve process efficiency. Some wastewater has been treated by FO/MD hybrid system, such as domestic wastewater [16,17], strong industrial wastewater [18–21], real human urine [22], and protein solutions [23]. However, few studies have been reported to reclaim real DWW by FO/MD hybrid system with commercial aquaporin (AQP) membrane. AQP membrane used for FO is a novel development, but AQP was early put forward by Agre [24]. Water can pass across biological cells through a group of transmembrane proteins known as AQPs, which is a natural desalination. The water transport channels of AQPs, which are like an hour glass, work extremely well in water delivery with excellent selectivity [24]. The current study provided the performance comparison between the thin film composite with embedded polyester screen support (TFC-ES) membrane and the AQP membrane. Moreover, reverse draw solute flux was not determined by conventional conductivity or salt concentration measurement but by the chlorine concentration monitoring. The specific reverse salt flux is adopted as an index to reflect the membrane filtration performance.

The focus of the investigation was on the performance comparison between the TFC-ES membrane and the AQP membrane in the FO/MD hybrid system to recycle real DWW. Lab-scale FO and FO/MD batch experiments were implemented, from which an analysis of the water flux, reverse draw solute flux, and contaminant rejections, as well as the specific reverse salt flux was conducted.

2. Materials and methods

2.1. Feed and draw solutions

Deionized (DI) water (in baseline experiments) and real DWW were used as the feed solutions (FS). DWW was taken from an industrial facility of dairy products, located at Hohhot, Inner Mongolia of China. Main indexes of DWW with precipitation are as follows: total organic carbon (TOC) of 595 ± 27.0 mg/L, total nitrogen (TN) of 71 ± 12.1 mg/L, and total phosphorous (TP) of 8.8 ± 1.77 mg/L. The DS was prepared with ACS grade sodium chloride (NaCl; Tianjin, China) dissolved in DI water.

2.2. FO and MD membranes

Two types of thin film composite FO membranes were the TFC-ES membrane (Hydration Technologies, Inc., Albany, OR, USA) and the AQP membrane (Sterlitech Corporation, Kent, WA, USA), respectively. Polytetrafluoroethylene (PTFE) membrane (Haining, Zhejiang, China) was used as the MD membrane. Characteristics of the membranes are displayed in Table 1. Quantachrome Instruments (Quadrasorb SI, USA) were employed to determine the pore sizes of the FO membranes through Horvath–Kawazoe method. A micrometer calipers measured the thicknesses of the FO membranes.

Table 1
Pore sizes and thicknesses of the FO membranes and MD membrane

	TFC-ES	AQP	PTFE
Pore size (nm)	0.452	0.368	450
Thickness (μm)	100–105	110–115	180–200
pH range	2–11	2–11	0–14
Maximum temperature (°C)	71	50	80
Salt rejection (%)	99.4	–	–

The pH range and maximum operating temperature of the FO membranes (as well as the characteristics of the PTFE membrane) were provided by manufacturers. The images of the TFC-ES and AQP membranes displayed in Fig. 1 were obtained from inVia Microscope Raman (RENISHAW, London, England).

2.3. Experimental setup

The FO/MD hybrid experimental system (Fig. 2) was a combination of a cross-flow FO cell and an air gap membrane distillation (AGMD) module. The effective membrane surface area of the FO cell was 90 cm^2. Two variable-speed peristaltic pumps (BT300-2J/YZ1515X-A, Longer, China) were employed to recirculate the FS and the DS. An AGMD cross-flow cell was designed as cylinder type, including a hot feed chamber and a cooling water chamber, as well as a 3-mm width air gap between them. Two pieces of PTFE membrane were fastened to opposite sides of a hot feed chamber. The AGMD module was composed of two hot chambers and three cooling water chambers. The total effective membrane area was 400 cm^2. Another two variable-speed peristaltic pumps (BT300-2J/YZ1515X-A, Longer, China) were used to transport the hot feed and the cooling water.

2.4. Experimental operation conditions

In the FO batch experiments, an FS beaker was placed on an electronic balance to calculate the water flux through the FO membrane. The chlorine concentration in the FS was measured by an ion chromatography system (DIONEX ICS-1100, USA) to determine the reverse draw solute flux. Initial volume of the FS and the DS was 2.0 L. Both the FS and the DS were cocurrently circulated at 0.5 L/min in the opposite channels of the FO cell. The experiments were operated at ambient temperature of 20°C ± 2°C. FO mode (active layer against feed solution) was adopted in all experiments.

The baseline experiment was run for 6 h. For DWW experiments, three cycles were run with each cycle of 6 h. The FO membrane was not cleaned until the third cycle finished. The FO membranes were cleaned in situ by osmotic backwashing (with sodium chloride against active layer and DI water against support layer) for 20 min, then DI water flushing (both sides) for 20 min. After membrane cleaning, recoverable water flux and reverse draw solute flux were measured. The concentrations of TOC, TN, and TP in the initial FS, initial DS, and final DS were measured.

In the FO/MD batch experiments, the concentration of the DS (1 M) could be kept constant by the AGMD module.

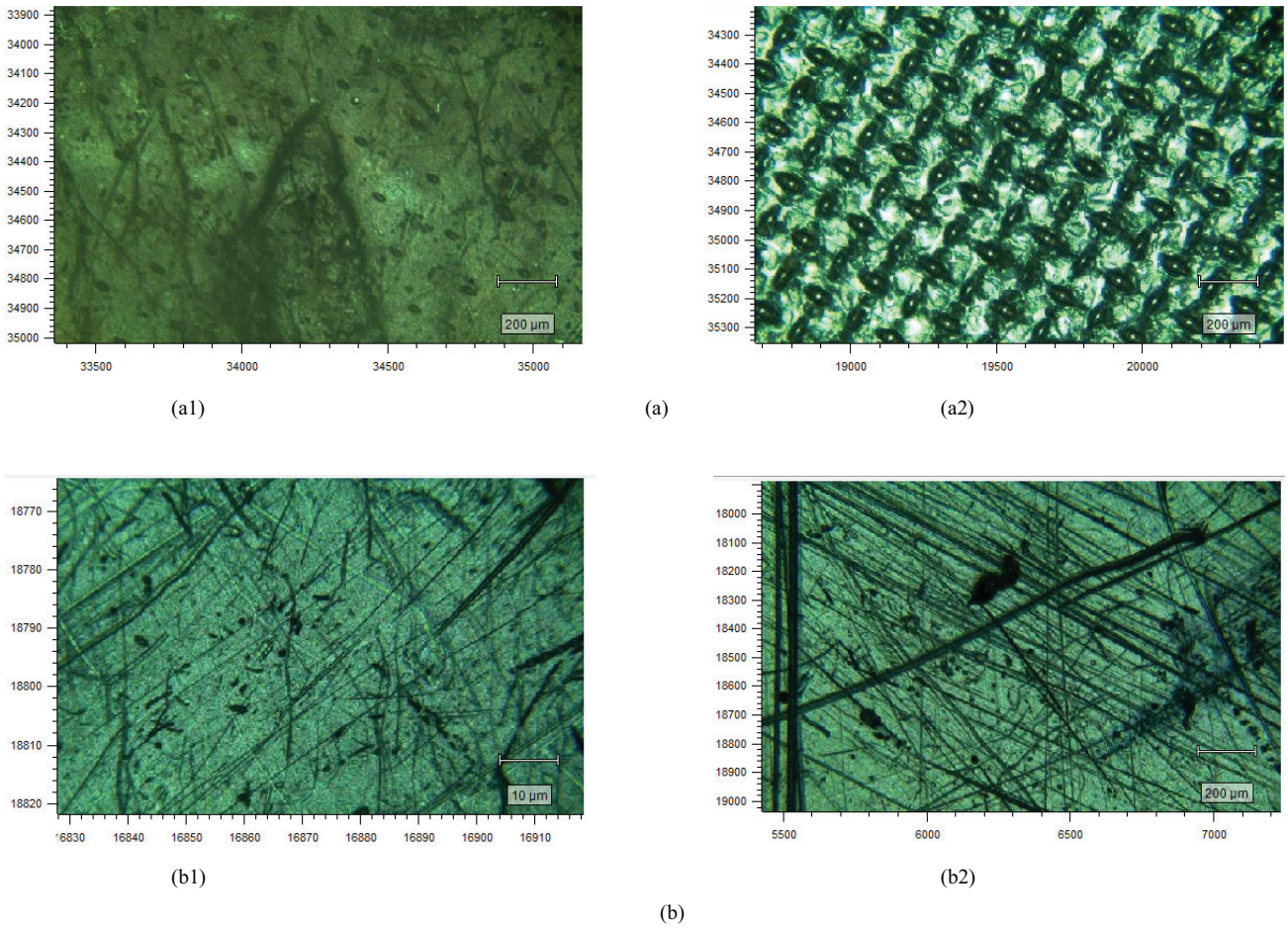

Fig. 1. Morphology of the (a) TFC-ES and (b) AQP membranes using inVia Microscope Raman. Images of the TFC-ES membrane: (a1) active layer surface and (a2) support layer surface. Images of the AQP membrane: (b1) active layer surface and (b2) support layer surface.

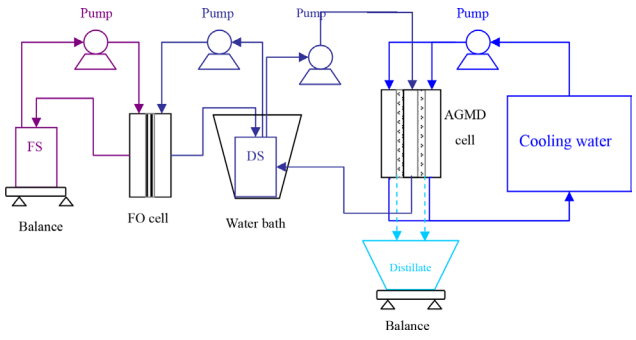

Fig. 2. Schematic diagram of the lab-scale FO/MD hybrid system.

The AGMD subsystem was driven by the transition temperature difference of 20°C–22°C. The DS could be held at 40°C in a water bath. The cooling water reservoir (approximately 100 L) maintained at 18°C–20°C. The hot DS and the cooling water were both circulated at 70 L/h. Permeate variations of the AGMD system were monitored to calculate the AGMD water flux. The concentrations of TOC, TN, and TP in the initial FS, as well as in the distillate, were analyzed for the contaminants rejection calculation. Additionally, conductivity, Na, Ca, Fe, protein, and polysaccharides of the distillate were measured.

2.5. Analytical methods

The concentrations of TOC and TN were analyzed by a TOC/TN analyzer (multi N/C 2100S, Analytik Jena, Germany), and the concentrations of COD and TP were measured by the Chinese NEPA standard methods (CEPB, 2002). Cl^- was detected by ion chromatography system (DIONEX ICS-1100, USA). Na, Ca, and Fe were examined by ICP-OES (OPTIMA 7000 DV, PerkinElmer, USA). Protein and polysaccharides concentrations were quantified by the Lowry method and the anthrone–sulfuric method, respectively, using ultraviolet spectrophotometer (UV-3150PC, Shimadzu, Japan).

The water flux was determined by the following equation:

$$J_W = \frac{\Delta V}{A \cdot \Delta t} \quad (1)$$

where J_W (L/m^2 h) is the water flux, ΔV (L) is the permeate volume through the membrane in the definite time intervals Δt (h), and A (m^2) is the effective membrane area.

Contaminant rejection R (%) was figured out by the following equation:

$$R = \left(1 - \frac{C_P}{C_{f,i}}\right) \times 100\% \quad (2)$$

where $C_{f,i}$ (mg/L) is the initial contaminant concentration in the FS (dairy wastewater), and C_P (mg/L) is the contaminant concentration in the distillate.

3. Results and discussion

3.1. FO batch experiments

3.1.1. Flux analysis

The water flux for the TFC-ES and AQP membranes are described in Figs. 3(a1) and (b1), respectively. The water flux for the TFC-ES membrane was higher than that of the AQP membrane. The DI water flux decrease ascribed to the diluted DS and the internal concentration polarization (ICP). The DWW flux decreased dramatically (Figs. 3(a1) and (b1)) mainly because of the occurrence of membrane fouling or the presence of pollutants in the DWW. Simultaneously, membrane fouling exacerbated ICP, resulting in the sharp flux decline. It seemed that the DWW flux decrements for the TFC-ES membrane were greater and faster than that of the AQP membrane. The reason was that the initial flux of the TFC-ES membrane was higher than that of the AQP membrane, leading to the suffering from fiercer subsequent effects of diluted DS, enhanced ICP and membrane fouling. From the TFC-ES membrane experiments, the water flux in the cycle DWW-2 was much lower than that in the cycle DWW-1 (Fig. 3(a1)), indicating that membrane fouling might be in the growing stage during the DWW-2. From the AQP membrane experiments shown in Fig. 3(b1), slight flux differences between the first cycle DWW-1 and the second cycle DWW-2 indicated that membrane fouling might emerge in the initial stage, and no visible cake layer formed during the cycle DWW-2. However, membrane fouling had been severe when the third cycle DWW-3 was completed. The AQP membrane surface may be modified by the organic and inorganic contaminants in the DWW during the first two cycles, and severe membrane fouling broke out in the third cycle.

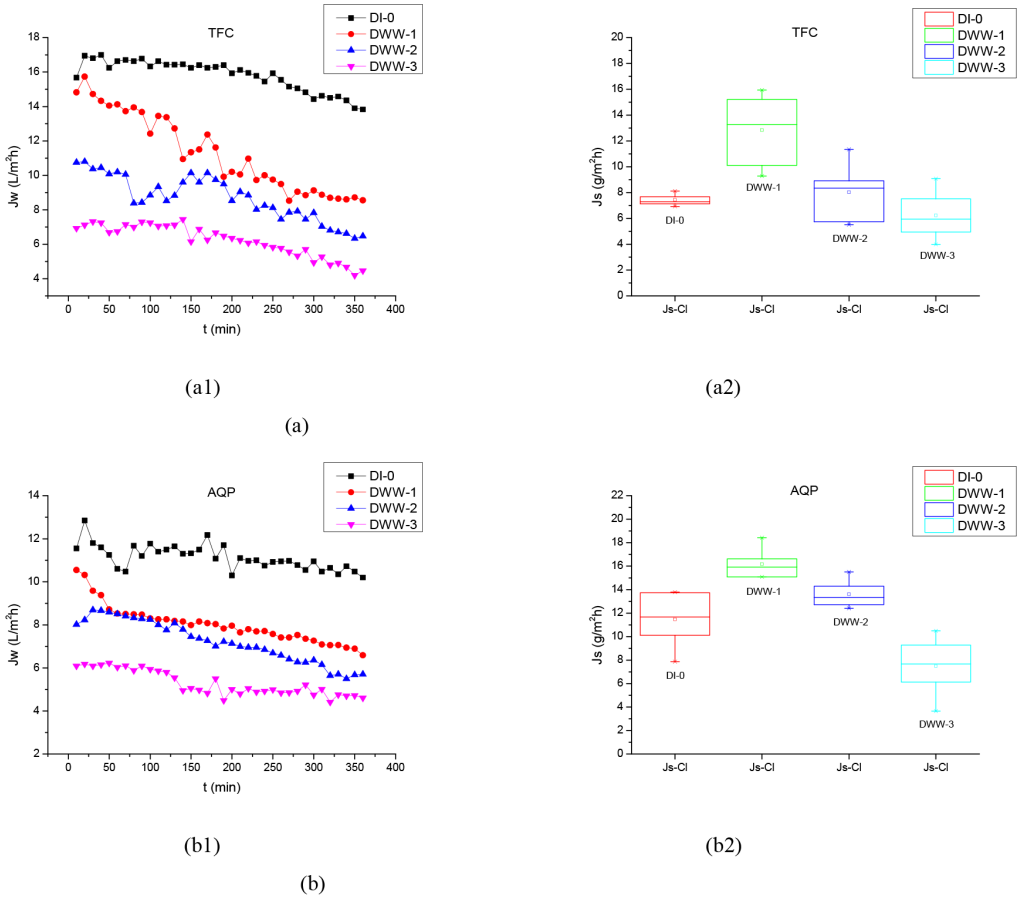

Fig. 3. Variations of the water flux (J_w (L/m² h)) with time (t (min)) and distribution of the reverse draw solute flux (J_s-Cl (g/m² h)) in the lab-scale FO batch experiments. DI-0 represents the baseline experiment. DWW-1, DWW-2, and DWW-3 refer to three cycles from 1 to 3 with DWW as the FS. In all FO experiments, NaCl solution (initial concentration of 1 M) was used as the DS. (a) FO experiments with the TFC-ES membrane: (a1) water flux and (a2) reverse draw solute flux. (b) FO experiments with the AQP membrane: (b1) water flux and (b2) reverse draw solute flux.

It can be seen from Figs. 3(a2) and (b2) that although the water flux was larger for the TFC-ES membrane than that for the AQP membrane, the reverse solute flux (RSF) for the TFC-ES membrane was smaller than that for the AQP membrane instead. Interestingly, the RSF varied inconsistently with the water flux trend, depending on the membrane properties. However, the less water flux variation happened during a cycle, the smaller range RSF varied over. As shown in Figs. 3(a2) and (b2), the RSF in the DWW experiment (DWW-RSF) for the TFC-ES membrane varied over a wider range than that for the AQP membrane except for the RSF in the baseline experiment (DI-RSF) because of the greater DWW flux variation for the TFC-ES membrane. In addition, although the DI water flux was higher than the DWW flux, the DI-RSF was not to be higher than the DWW-RSF. It is because that many molecules and ions in the DWW influenced the charged characteristics of the FO membranes by adsorption, which led to stronger electrostatic interactions for chlorine ions, accordingly higher DWW-RSF. The RSF of DWW-1 and DWW-2 was higher than that of DI-RSF, suggesting that light membrane fouling or foulants of the DWW modified the membrane surface property and increased the RSF while severe membrane fouling (DWW-3) decreased the RSF because of the membrane fouling layer resistance. Also seen from Figs. 3(a2) and (b2), the DWW-RSF declined gradually from the first cycle to the third cycle, which illustrated that the DWW-RSF decreased with the evolution of membrane fouling. However, whether the DWW-RSF can be lower than the DI-RSF depends on the overall effects between the electrostatic strength and the resistance of the fouling layer. As shown in Figs. 3(a2) and (b2), the RSF of DWW-3 was lower than that of the DI-RSF, which inferred that the hindrance of membrane fouling had been stronger than the electrostatic attraction. With the FS being concentrated and the DS being diluted, many ions can accumulate with the contaminants on the fouling layer leading to the existence of the electrostatic repulsion towards diluted chlorine ions in the DS. From another point of view, the membrane fouling extent had been more severe for the AQP membrane than that for the TFC-ES membrane when the third cycle was completed.

3.1.2. Contaminant rejections

Results in Table 2 show that the contaminant (TOC, TN, and TP) rejections for the AQP membrane were slight lower than that of the TFC-ES membrane. The pore size of the AQP membrane is smaller than that of the TFC-ES membrane (shown in Table 1) and so size exclusion for contaminants was stronger, and a higher rejection took place with the AQP membrane. The TP rejection was higher than the TN and TOC rejections, and reached over 99%, because phosphates were negatively charged and had a larger hydrated radius. The TN rejection was the lowest. One reason may be that ammonia is positively charged and has a relatively small hydrated radius. Another, small organic molecule, such as urea, cannot be rejected well. In addition, the contaminant rejections in Table 2 were observed to increase gradually from the cycle DWW-1 to DWW-3 – that is, membrane fouling, which ranged from mild to severe. Rejections may be higher on a fouled membrane [25] because a fouled membrane can reduce mass transport capacity, and elevate electrostatic repulsion on the membrane surface. Consequently, membrane fouling hampered contaminant passage through the membrane.

3.1.3. Specific reverse salt flux and recoverable water flux

The specific reverse salt flux (J_s/J_w), recoverable water flux (J_w') of the fouled membrane, water permeability (A), and solute permeability (B) of two membranes are shown in Table 3. RO experiments [26] were performed to get A and B values of the AQP membrane. A and B values of the TFC membrane were cited from Lutchmiah et al. [10]. A value can be calculated by the equation: $J_w = A \cdot \Delta p$, B value by the equation: $J_s = B \cdot \Delta C$. From Table 3, A value of the AQP membrane is larger than that of the TFC membrane, and B value

Table 2
TOC, TN, and TP rejections for the FO experiments

Rejections (%)	FO experiments					
	TFC-ES membrane			AQP membrane		
	DWW-1	DWW-2	DWW-3	DWW-1	DWW-2	DWW-3
TOC	96.33	97.01	97.85	97.8	97.8	98.03
TN	93.43	95.28	96.05	96.25	96.45	97.11
TP	99.53	99.56	99.65	99.59	99.59	99.71

Table 3
Indexes of the FO membranes in the FO batch experiments

FO index Membrane	DI water flux, J_w (L/m² h)	Recoverable water flux, J_w' (L/m² h)	J_w'/J_w (%)	J_s/J_w (mol/L)	J_s'/J_w' (mol/L)	A (10^{-12} m/s Pa)	B (10^{-7} m/s)
TFC-ES	16.57	15.21	91.79	0.0100	0.0211	3.18–9.60	0.02–47.20
AQP	12.16	9.89	81.33	0.0218	0.0319	21.22	39.47

Note: The data were the averages within 2 h. A and B values of the AQP membrane are from the RO experiments. A and B values of the TFC membrane are given by Lutchmiah et al. [10].

is also larger than most values of the TFC membrane except one maximum. Besides, 91.79% of the cleaned TFC-ES membrane water flux was recovered, and 81.33% of the rinsed AQP membrane water flux was also recovered, suggesting that reversible membrane fouling accounted for a larger part on the TFC-ES membrane than that on the AQP membrane. The specific RSF (J_s/J_w) and recoverable value (J_s'/J_w') for the TFC-ES membrane were both lower than the AQP membrane. A simple cleaning method (osmotic backwashing and water flushing in situ) is effective for the FO membrane flux recovery in the DWW treatment.

3.2. FO/MD batch experiments

3.2.1. Flux analysis

The variations of the water flux and the RSF in the FO subsystem of the hybrid system are displayed in Fig. 4. As shown in Figs. 4(a1) and (b1), in the hybrid system, the FO water flux for the TFC-ES membrane was still higher than that of the AQP membrane. The FO water flux varied mildly during each cycle except for initial variations in the start-up of each experiment, indicating that the osmotic pressure difference was relatively stable in the five-sixths cycle, owing to DS being undiluted by the AGMD subsystem. Moreover, the build-up of the hybrid system mitigated the membrane fouling and ICP for its mesophilic operating temperature. As for the significant FO water flux fluctuations in the initial stage of a cycle, the membrane fouling and the ICP were inevitably the key factor. With respect to the RSF, cases from Figs. 4(a2) and (b2) were similar to that from Figs. 3(a2) and (b2). Comparing the water flux in Figs. 3(a1) and (b1) with that in Figs. 4(a1) and (b1), the FO water flux was higher in the FO/MD hybrid system than that in the FO system, owing to the thermal DS with constant concentration remained by the MD subsystem.

3.2.2. Contaminant rejections

The results of the contaminant rejections (listed in Table 4) show that rejection of the TOC, TN, and TP in the FO/MD hybrid system was over 99%. The rejection of TP even reached

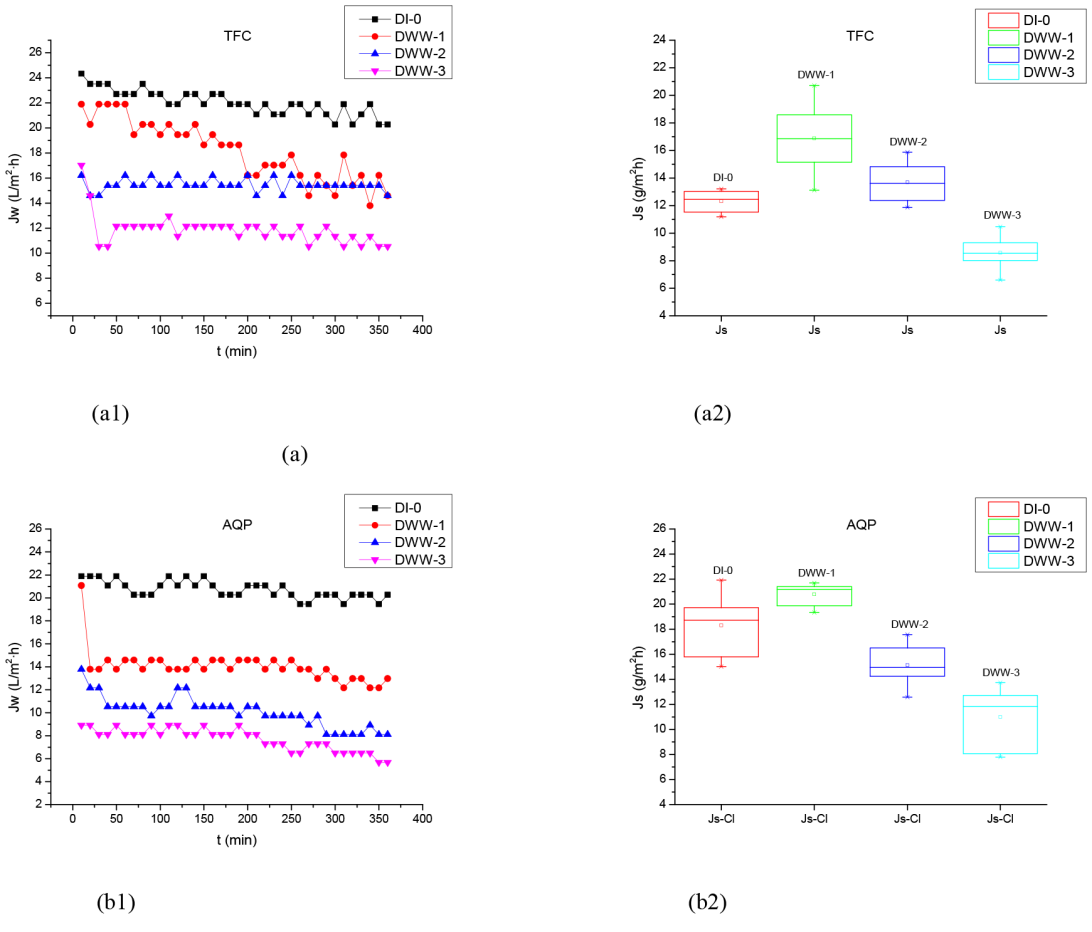

Fig. 4. Variations of the FO water flux (J_w (L/m² h)) with time (t (min)) and distribution of the FO reverse draw solute flux (J_s-Cl (g/m² h)) in the lab-scale FO/MD batch experiments. DI-0 represents the baseline experiment with DI water as the FS. DWW-1, DWW-2, and DWW-3 refer to the cycles from 1 to 3 with the DWW as the FS. In all FO/MD experiments, NaCl solution (initial concentration of 1 M) was used as the DS. (a) FO/MD experiments with the TFC-ES membrane: (a1) water flux in the FO subsystem and (a2) reverse flux in the FO subsystem. (b) FO/MD experiments with the AQP membrane: (b1) water flux in the FO subsystem and (b2) reverse flux in the FO subsystem.

100%, and TN was the lowest. A miniscule reduction of each contaminant rejection was observed from the cycle DWW-1 to DWW-3, one cause of which was wetting and fouling in the MD membrane. The AQP membrane reached a slightly higher level of contaminant rejection than the TFC-ES membrane did.

3.2.3. Characteristics of the distillate by the FO/MD hybrid system

The MD water rates are listed in Table 5. Characteristics of the distillate are presented in Table 6. The distillate from the hybrid system using the AQP membrane was preferable to that from the hybrid system using the TFC-ES membrane. However, no matter which FO membrane was used, the permeate water quality from the hybrid system was both higher than water quality standard for urban miscellaneous water consumption of China (GBT18920-2002).

3.2.4. Specific reverse salt flux

The values of the specific RSF (J_s/J_w) are shown in Fig. 5 to further distinguish the performance of the FO membranes in the reclamation of DWW. The lower specific RSF, meaning favorable membrane selectivity, is expected [10]. The reference value of the specific RSF can be calculated according to the existing data given by Lutchmiah et al. [10]. For the thin film composite membrane, the maximum value of the specific RSF was 0.09467 mol/L (T = 40°C, the MD operation temperature) which, compared with the results from Fig. 5, the specific RSF of the TFC-ES membrane and the AQP membrane, was in accordance with the calculated references. And clearly, the specific RSF of the TFC-ES membrane was much lower and more invariable than that of the AQP membrane.

4. Conclusion

The study confirms that the FO/MD hybrid system is effective in the reclamation of DWW with high-quality product water for miscellaneous urban water reuse. The TFC-ES and AQP membranes performed well in DWW treatment. The TFC-ES membrane had higher levels of water flux, lower RSF, lower specific RSF and higher flux recovery for DWW treatment and recycling than the AQP membrane. The AQP membrane exhibited slight higher contaminant rejections than the TFC-ES membrane did in the FO experiments.

Acknowledgments

This study was financially supported by the Natural Science Foundation of Inner Mongolia (No. 2017MS0216); the Department of Education of Inner Mongolia Autonomous Region (No. NJZY17095). The author would like to thank Ryan W. Holloway and Keith Lampi for their help.

Table 6
Characteristics of the distillate vs. DWW in the FO/MD experiments

Characteristics	Distillate		DWW
	TFC-ES	AQP	
Total organic carbon (mg/L)	3.80	1.09	595 ± 27.0
Total nitrogen (mg/L)	0.641	0.496	71 ± 12.1
Total phosphorous (mg/L)	0.011	0.005	8.8 ± 1.77
Protein (mg/L)	0.368	0.315	90 ± 3.8
Polysaccharides (mg/L)	11.954	10.895	1,484 ± 20.3
pH	6.69	6.71	8.0–9.0
Conductivity (μs/cm)	13.58	17.7	1,021 ± 29.8
Na (mg/L)	2.919	3.100	68 ± 2.9
Ca (mg/L)	0.262	0.288	26 ± 0.36
Fe (mg/L)	0.000	0.000	0.42 ± 0.024
Cl^- (mg/L)	6.035	5.785	113 ± 31.0

Table 4
TOC, TN, and TP rejections for the FO/MD experiments

Rejections (%)	FO/MD experiments					
	TFC-ES membrane			AQP membrane		
	DWW-1	DWW-2	DWW-3	DWW-1	DWW-2	DWW-3
TOC	99.49	99.40	99.21	99.86	99.81	99.26
TN	99.22	99.10	99.01	99.31	99.20	99.11
TP	100	100	99.89	100	100	99.92

Table 5
Water rates between FO and MD subsystems for the FO/MD experiments

Subsystem	Water rate (L/h)					
	TFC-ES membrane			AQP membrane		
	DWW-1	DWW-2	DWW-3	DWW-1	DWW-2	DWW-3
FO	0.16	0.13	0.11	0.12	0.08	0.06
MD	0.13	0.12	0.10	0.12	0.11	0.10

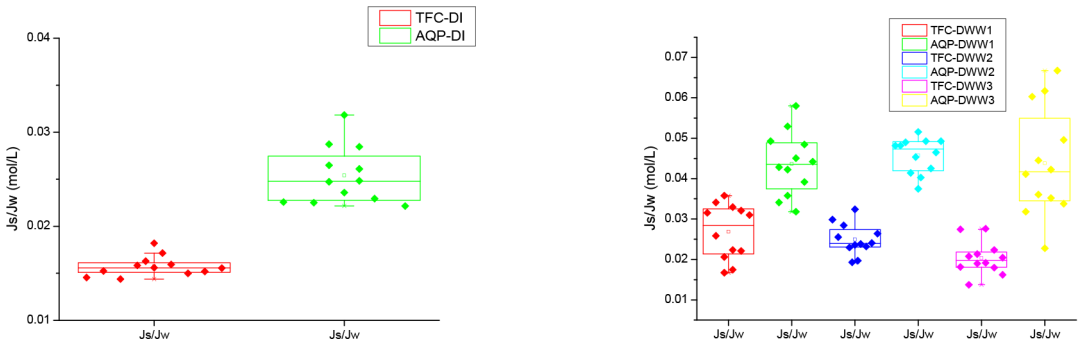

(a) (b)

Fig. 5. Specific RSF (mol/L) distribution for the TFC-ES and AQP membranes in the lab-scale FO/MD batch experiments. DI represents the baseline experiment. DWW-1, DWW-2, and DWW-3 refer to the cycles from 1 to 3 with DWW as the FS. In all experiments, NaCl solution (initial concentration of 1 M) was used as the DS. Specific RSF of the (a) baseline experiments and (b) DWW experiments.

Disclosure statement

No potential conflict of interest was reported by the authors.

References

[1] S.F. Magram, A review on membrane technologies and associated costs for municipal wastewater reuse, Int. J. Chem. Technol., 1 (2009) 33–43.
[2] A.K. Slavov, General characteristics and treatment possibilities of dairy wastewater – a review, Food Technol. Biotechnol., 55 (2017) 14–28.
[3] X. Zheng, Z.X. Zhang, D.W. Yu, X.F. Chen, R. Cheng, S. Min, J.Q. Wang, Q.C. Xiao, J.H. Wang, Overview of membrane technology applications for industrial wastewater treatment in China to increase water supply, Resour. Conserv. Recycl., 105 (2015) 1–10.
[4] J.R. McCutcheon, M. Elemelech, Influence of concentrative and dilutive internal concentration polarization on flux behavior in forward osmosis, J. Membr. Sci., 284 (2006) 237–247.
[5] T.Y. Cath, A.E. Childress, M. Elimelech, Forward osmosis: principles, applications, and recent developments, J. Membr. Sci., 28 (2006) 70–87.
[6] A. Alkhudhiri, N. Darwish, N. Hilal, Membrane distillation: a comprehensive review, Desalination, 287 (2012) 2–18.
[7] Q.H. She, R. Wang, A.G. Fane, C.Y.Y. Tang, Membrane fouling in osmotically driven membrane processes: a review, J. Membr. Sci., 499 (2016) 201–233.
[8] B.D. Coday, P. Xu, E.G. Beaudry, J. Herron, K. Lampi, N.T. Hancock, T.Y. Cath, The sweet spot of forward osmosis: treatment of produced water, drilling wastewater, and other complex and difficult liquid streams, Desalination, 333 (2014) 23–35.
[9] R.V. Linares, Z. Li, S. Sarp, S.S. Bucs, G. Amy, J.S. Vrouwenvelder, Forward osmosis niches in seawater desalination and wastewater reuse, Water Res., 66 (2014) 122–139.
[10] K. Lutchmiah, A.R.D. Verliefde, K. Roest, L.C. Rietveld, E.R. Cornelissen, Forward osmosis for application in wastewater treatment: a review, Water Res., 58 (2014) 179–197.
[11] D.L. Shaffer, J.R. Werber, H. Jaramillo, S. Lin, M. Elimelech, Forward osmosis: where are we now? Desalination, 356 (2015) 271–284.
[12] L. Chekli, S. Phuntsho, J.E. Kim, H.K. Shon, A comprehensive review of hybrid forward osmosis systems: performance, applications and future prospects, J. Membr. Sci., 497 (2016) 430–449.
[13] Q. Yang, J. Lei, D.D. Sun, D. Chen, Forward osmosis membranes for water reclamation, Sep. Purif. Rev., 45 (2016) 93–107.
[14] A.J. Ansari, F.I. Hai, W.E. Price, L.D. Nghiem, Forward osmosis as a platform for resource recovery from municipal wastewater – a critical assessment of the literature, J. Membr. Sci., 529 (2017) 195–206.
[15] M.S. El-Bourawi, Z. Ding, R. Ma, M. Khayet, A framework for better understanding membrane distillation separation process, J. Membr. Sci., 285 (2006) 4–29.
[16] T. Husnain, Y.L. Liu, R. Riffat, B.X. Mi, Integration of forward osmosis and membrane distillation for sustainable wastewater reuse, Sep. Purif. Technol., 156 (2015) 424–431.
[17] T. Husnain, B. Mi, R. Riffat, Fouling and long-term durability of an integrated forward osmosis and membrane distillation system, Water Sci. Technol., 72 (2015) 2000–2005.
[18] Q.C. Ge, P. Wang, C.F. Wan, T.S. Chung, Polyelectrolyte-promoted forward osmosis–membrane distillation (FO–MD) hybrid process for dye wastewater treatment, Environ. Sci. Technol., 46 (2012) 6236–6243.
[19] X.M. Li, B.L. Zhao, Z.W. Wang, M. Xie, J.F. Song, L.D. Nghiem, T. He, C. Yang, C.X. Li, G. Chen, Water reclamation from shale gas drilling flow back fluid using a novel forward osmosis–vacuum membrane distillation hybrid system, Water Sci. Technol., 69 (2014) 1036–1044.
[20] M. Xie, L.D. Nghiem, W.E. Price, M. Elimelech, A forward osmosis–membrane distillation hybrid process for direct sewer mining: system performance and limitations, Environ. Sci. Technol., 47 (2014) 13486–13493.
[21] S. Zhang, P. Wang, X.Z. Fu, T.S. Chung, Sustainable water recovery from oily wastewater via forward osmosis–membrane distillation (FO–MD), Water Res., 52 (2014) 112–121.
[22] Q.L. Liu, C.H. Liu, J. Ma, et al., Integrated forward osmosis–membrane distillation process for human urine treatment, Water Res., 91 (2016) 45–54.
[23] K.Y. Wang, M.M. Teoh, A. Nugroho, T.S. Chung, Integrated forward osmosis-membrane distillation (FO-MD) hybrid system for the concentration of protein solutions, Chem. Eng. Sci., 66 (2011) 2421–2430.
[24] P. Agre, Aquaporin water channels, Biosci. Rep., 24 (2004) 127–163.
[25] R. Valladares Linares, V. Yangali-Quintanilla, Z.Y. Li, G. Amy, Rejection of micropollutants by clean and fouled forward osmosis membrane, Water Res., 45 (2011) 6737–6744.
[26] B. Kim, G. Gwak, S. Hong, Review on methodology for determining forward osmosis (FO) membrane characteristics: water permeability (A), solute permeability (B), and structure parameter (S), Desalination, 422 (2017) 5–16.